

Video Article

Applying X-ray Imaging Crystal Spectroscopy for Use as a High Temperature Plasma Diagnostic

Norman M. Cao¹, Andrés M. Mier Valdivia², John E. Rice³¹Department of Nuclear Science and Engineering, Massachusetts Institute of Technology²Department of Physics, Massachusetts Institute of Technology³Plasma Science and Fusion Center, Massachusetts Institute of TechnologyCorrespondence to: John E. Rice at rice@psfc.mit.eduURL: <http://www.jove.com/video/54408>DOI: [doi:10.3791/54408](https://doi.org/10.3791/54408)

Keywords: Engineering, Issue 114, X-Ray Spectroscopy, Crystal Spectroscopy, Plasma Physics, Fusion, Tokamaks, Plasma Diagnostics

Date Published: 8/25/2016

Citation: Cao, N.M., Mier Valdivia, A.M., Rice, J.E. Applying X-ray Imaging Crystal Spectroscopy for Use as a High Temperature Plasma Diagnostic. *J. Vis. Exp.* (114), e54408, doi:10.3791/54408 (2016).

Abstract

X-ray spectra provide a wealth of information on high temperature plasmas; for example electron temperature and density can be inferred from line intensity ratios. By using a Johann spectrometer viewing the plasma, it is possible to construct profiles of plasma parameters such as density, temperature, and velocity with good spatial and time resolution. However, benchmarking atomic code modeling of X-ray spectra obtained from well-diagnosed laboratory plasmas is important to justify use of such spectra to determine plasma parameters when other independent diagnostics are not available. This manuscript presents the operation of the High Resolution X-ray Crystal Imaging Spectrometer with Spatial Resolution (HIREXSR), a high wavelength resolution spatially imaging X-ray spectrometer used to view hydrogen- and helium-like ions of medium atomic number elements in a tokamak plasma. In addition, this manuscript covers a laser blow-off system that can introduce such ions to the plasma with precise timing to allow for perturbative studies of transport in the plasma.

Video Link

The video component of this article can be found at <http://www.jove.com/video/54408/>

Introduction

X-ray spectra provide a wealth of information on high temperature plasmas; for example electron temperature and density can be inferred from line intensity ratios. By using a Johann spectrometer viewing the plasma off-axis, it is possible to construct profiles of plasma parameters such as density, temperature, and velocity inside the plasma with good spatial and time resolution^{1,2}. This manuscript presents the operation of the High Resolution X-ray Crystal Imaging Spectrometer with Spatial Resolution (HIREXSR), a high wavelength resolution spatially imaging X-ray spectrometer used to view hydrogen- and helium-like ions of medium atomic number elements in a tokamak plasma.

HIREXSR is deployed on Alcator C-Mod, a tokamak fusion device with a major and minor radius of 0.67 m and 0.22 m respectively. It typically operates with deuterium plasmas lasting ~2 sec with average densities between $0.2\text{--}8.0 \times 10^{20} \text{ m}^{-3}$ and central electron temperatures between 1-9 keV³. Under these conditions, medium to high Z impurity elements become highly ionized and radiate in the X-ray range, which HIREXSR measures. Benchmarking atomic code modeling of X-ray spectra obtained from well-diagnosed laboratory plasmas is important to justify use of such spectra to determine plasma parameters when other independent diagnostics are not available⁴.

Every spectrometer is built for its desired use. Accordingly, a general description about the machine and its related concepts is necessary to fully comprehend these powerful tools⁵. Bragg reflection occurs when a photon reflects off adjacent layers of a crystal and travels a distance that is a multiple of its wavelength. **Figure 1** depicts this phenomenon. This condition is expressed by the equation $n\lambda = 2d \sin \theta_b$, where n is the order of reflection, λ is the wavelength of the photon, d is the separation between adjacent layers of the crystal and θ_b is the Bragg angle. A one to one correspondence between λ and θ_b indicates that all photons at a specific point of the detector plane travel with the same wavelength. In practice, however, absorption and precision limitations manifest as a deviation from the Bragg angle. This results in only a small range of angles that produce significant constructive interference, represented by a rocking curve⁶. **Figure 2** is an example curve for a calcite crystal.

HIREXSR is a Johann spectrometer with a spherically bent crystal⁷. Before describing this kind of device, a discussion of a simpler, circular spectrometer is appropriate. This set up consists of a bent crystal that reflects incoming photons at their respective Bragg angles towards an array of single X-ray photon counting pixel detectors. The crystal and the detector lay tangent to the Rowland circle, as displayed in **Figure 3**. The diameter of the Rowland circle is equal to the radius of curvature of the crystal. All rays from a given point on the circumference to any point on the crystal have the same incident angle with respect to the crystal itself.

In the case of HIREXSR, a spherically bent crystal permits spatial resolution in the meridional plane, illustrated in **Figure 4**. The meridional focus f_m is defined as: $f_m = R_c \sin \theta_b$, where R_c is the radius of curvature of the crystal. The sagittal focus f_s is defined as: $f_s = -f_m / \cos 2\theta_b$. The spatial

resolution of the spectrometer Δx is given by: $\Delta x = \frac{|f_s - L_{cp}|d}{f_s}$, where L_{cp} is the distance between the crystal and the plasma, and d is the height of the crystal. Because the 2-dimensional spacing of the crystal layers is discrete, this must be taken into consideration when choosing a material. Since the detector surfaces are planar, they can only be tangent to the Rowland circle at one point, which consequently gives rise to error since the detected rays are not landing precisely on their corresponding points on the Rowland circle. Physically, this misalignment manifests as a "smearing" of photons of specific energy on the detector. This Johann error is defined as $\delta x_j = \frac{l^2 \cos \theta_b}{8R_c}$, where l is the width of the crystal. If the detector pixel width δx_p is much larger than the Johann error, then the spectral resolution is independent of it. If they are of comparable size, then the total error can be approximated by $\delta x \approx \sqrt{\delta x_j^2 + \delta x_p^2}$. The resolving power of the crystal spectrometer is given by: $\frac{\lambda_0}{\Delta \lambda} = \frac{\tan \theta_b}{\delta \theta}$, where $\delta \theta = \frac{\delta x}{f_m}$. Instead of placing the detector tangent to a point on the Rowland circle however, in HIREXSR the detector is angled slightly to sacrifice accuracy for spectral range, as shown in **Figure 5**. This error analysis has been experimentally verified and conforms to expectation⁸.

There are two crucial parameters to consider when designing a Johann spectrometer. First, the imaging range determines what the spectrometer will be observing. For studying plasmas, it is highly desirable to view its entire cross section in order to distinguish between line shifts caused by poloidal and toroidal rotation. HIREXSR is mounted such that it can view the whole plasma, and is tilted slightly off-axis by #8° (illustrated in **Figure 6**) to allow for accurate toroidal measurements. Second, time resolution regulates the minimum time between events that the spectrometer can record. For Alcator C-Mod, desirable values are below 20 msec, shorter than the energy and particle confinement times. The X-ray counting pixel detectors that HIREXSR uses can support a time resolution of 6 to 20 msec or larger⁹. **Table 1** summarizes all of the module specifications.

For perturbative plasma studies, the laser blow-off system on Alcator C-Mod is used to deliver multiple ablations with precise timing¹⁰. The laser is a Nd:YAG (neodymium-doped yttrium aluminum garnet) operating at up to 10 Hz. The laser is incident on a remote-controlled optical train as shown in **Figure 7** that focuses and steers the beam to the desired location on the slide. Spot sizes of the laser need to be controlled so the injection doesn't disrupt the plasma. A long focal length (1,146 mm) converging lens is translated along the optical axis via a remote controlled linear stage to allow ablated spot sizes to vary from #0.5 to 7 mm. Fast beam steering is achieved via a 2D piezoelectric mirror. This piezoelectric system is mounted to an RS232 driven mirror mount capable. In addition to the Nd:YAG laser, a 633 nm diode laser is used to indicate the location of the main (infrared) beam. The beams are made to be collinear through the first mirror.

Protocol

1. Choosing Appropriate Spectral Lines

1. Choose appropriate emission lines that will determine the quality of obtained data. **Figure 8** shows which noble gas emission lines will be relevant at different values for the electron temperature.
 1. Note that the ionization state and line ratios are determined by the competition of ionization, collisional excitation, radiative recombination and dielectric recombination. These processes can vary with plasma temperature and density. See **Figure 9** for an example of this variation.
2. Refer to other published works for the wavelengths and relative strengths of emission lines of interest. In this protocol, use medium Z He-like ions as characterized in Rice, J. E. *et al.* (2015)⁴. See **Figure 10** for an example spectrum.
3. Note that it is important to study satellites from lines outside the main series, as they could be unresolved with the lines that are being measured. Some intrinsic impurities (Fe, Mo, Ti, etc.) will always be present from plasma-facing structure and components in the tokamak. For example, **Figure 11** suggests argon Ly_{α1} is a better choice than the Ly_{α2} line since the latter overlaps with a molybdenum line.
4. For plasmas in temperature ranges around 0.5-3 keV, capture the following He-like lines for argon (all from n = 2 transitions): resonance (w, 1s²S₀ - 1s2p ¹P₁), forbidden (z, 1s²S₀ - 1s2p ³S₁), and intercombination (x, 1s²1S₀ - 1s2p ³P₂ and y, 1s²1S₀ - 1s2p ³P₁). For argon n = 2 transitions, the H-like spectrum lies between 3.72 # < λ < 3.80 # and the He-like spectrum lies between 3.94 # < λ < 4.00 #. See **Figure 11** and **Figure 12** for plots of these spectra.

2. Mounting the HIREXSR Hardware

1. Refer to the relevant published works for the details and specifics on mounting and building HIREXSR^{1,2,5}. This section will focus on the most important and critical steps in that procedure.
2. Mount HIREXSR on one of the racetrack-shaped ports of Alcator C-Mod, angled to allow for an 8° off-diagonal view.
3. Obtain a circular (102)-quartz crystal with a 4.56215 # 2d spacing, a 50 mm diameter, and a 1,385 mm radius of curvature to view the H-like spectrum.
4. Obtain a rectangular (102)-quartz with a 4.56215 # 2D spacing, a width of 64 mm and a height of 27 mm to view the He-like spectrum.
5. Insert and mount both crystals within the housing of HIREXSR by accessing the spectrometer's housing through the hatch located on its side. See **Figure 13** for their layout.
6. Through the same hatch, bolt the four detectors on the designated movable mounts in the spectrometer body, reserving one detector for the H-like spectrum, and the other three for the He-like spectrum. This arrangement is illustrated in **Figure 14**.
7. Position the mounts 125 cm away from the crystals such that the line from the center of the crystals to that of the detectors makes an angle $\theta_b/2$ with the line from the center of the Rowland circle to the center of the crystal, where θ_b is the Bragg angle of the center of the spectrum being measured. See **Figure 5**.
 1. Note that for argon, the H-like crystal used results in $\theta_b = 55.5^\circ$, and the He-like crystal used results in $\theta_b = 60.5^\circ$.
8. Angle the detectors to match the modified arrangement illustrated in **Figure 5**.

1. Note that the precise alignment of the detectors is not important, as the collected data will be calibrated against a known source during the experimental run.
9. Separate HIREXSR's helium atmosphere from the tokamak vacuum by installing a 0.001" thick and 4" diameter beryllium window. See **Figure 13** for its layout.
10. Install a 10" gate valve between the window and reactor to protect against failure of the beryllium window.
 1. Note that the gate valve should close when the local pressure rises above 10 mTorr to avoid damage to both the spectrometer and the tokamak.
11. Refer to **Figure 6** and **Figure 15** for top-down and side views, respectively, of HIREXSR and Alcator C-Mod, along with relative distances of the detectors and crystals, and between the spectrometer and tokamak.

3. Setting Up the Laser Blow-off (LBO) System

1. Refer to the relevant published works for the details and specifics on the construction of the laser blow-off apparatus¹⁰.
2. To inject calcium, take a 2 μm CaF_2 slide with 100 \AA of chromium (to aid in laser absorption in the material) and place the slide in the laser blow-off system. As this requires access to the C-Mod reactor, do this before operations begin for the day.
3. Change to channel 14 on Alcator C-Mod's closed-circuit cable TV system to view a black and white CCD camera that watches the slide. The 633 nm diode laser spot should be visible on the slide.

4. Running a Plasma Experiment

1. At the beginning of the run day, start the script that will collect and save data from the X-ray counting pixel detectors for each experimental run, or "shot". This will depend on the specific detector setup in place. The steps specific to HIREXSR are presented here.
 1. From a workstation in the C-Mod control room, bring up a command line terminal.
 2. Connect to a detector remotely by entering "ssh -X det@dec0xx", where xx ranges from 07-10.
 3. Change directories by entering "cd p2_1mod"
 4. Run the command "runtvx". This will bring up a window that will avalanche with text.
 5. Once the text stops, press enter twice. The startup script will set the frame rate to 50 Hz and threshold energy to ~2 keV. Another avalanche of text will happen and the detectors will begin calibrating.
 6. Wait until all of this ends, and enter "exit" in the window.
 7. Repeat for each detector 07-10.
2. Throughout the day, maintain a helium atmosphere in HIREXSR slightly above ambient temperature by continuously pumping the gas into the housing for the duration of the operation. This reduces atmospheric X-ray attenuation and thermal expansion of the crystal.
3. Collaborate with on-site engineering staff to ensure the plasma reaches the desired plasma parameters during the upcoming shot. If the parameters are to change from shot to shot, communicate this to the engineering staff between every shot.
 1. Additionally, sometime during the run day, request a "locked mode" shot from the engineering staff for calibration of data taken that day. See Reinke *et al.* 2012¹ for an explanation of locked modes and how they are used for calibration.
4. For perturbative transport studies: Before each shot, program the laser blow-off system to inject the desired concentration of non-recycling impurities (CaF_2 , Sc, *etc.*) into the plasma at desired times.
 1. Decide on a laser spot size, which controls the amount of material ablated from the slide. From operational experience at Alcator C-Mod, roughly 10% of the ablated material makes it into the plasma core during low power operation¹⁰. Typical spot sizes range from 0.5 to 3.5 mm.
 2. Determine the desired blow-off timings, keeping in mind the maximum 10 Hz operation speed.
 3. Enter the desired spot size and timings to the laser blow-off system control GUI. For example, the transport study by Rice *et al.* 2013¹¹ varied the spot sizes from 0.5 to 3.5 mm and had injections every 300 msec.
5. For all studies: Set the gas valve to puff argon into the plasma 0.3 sec after the plasma starts. The puff should last about 0.1 sec and raise the argon density to about 10^{-4} times the electron density.
6. Use dwscope to view live diagnostic data during the run day for systems using MDSplus, such as C-Mod.
 1. From a workstation in the tokamak control room, open dwscope from the application menu
 2. Obtain one or more scope files with relevant diagnostics shown from another user, or create custom ones using the MDSplus Tree Command Language (advanced).
 3. Click "Customize | Use Saved Settings From..." and select a scope file to load it. A useful example scope, plasma_n_rot_z.dat, is shown with the dwscope GUI in **Figure 16**.
 4. Leave the textbox in the bottom bar blank and data will be loaded from the most recent shot.
 5. If desired, enter a shot number and click "Apply" to load data from a specific shot.
7. Inform the engineering operators that all preparations for the upcoming shot are complete and that they may proceed to ignite the plasma.
8. Wait for the operators to initiate the plasma and for it to end. In Alcator C-Mod, the initiation process will last around 3 min and the plasma will burn for less than 10 sec.
 1. If using the laser blow-off system, visually confirm slide ablation via the camera view of the slide (refer to Section 3).
9. Wait for the tokamak to cool in order to proceed to the next shot. In Alcator C-Mod, this process will last 10-15 min.
 1. Use this time to make any changes to the experimental set up and communicate them to the operators so they can be applied subsequently, if desired.

10. Note that if any changes to the hardware are desired, the researchers should request a "cell access" to the operators, during which they will open the tokamak and disengage other safety features to allow people to enter Alcator C-Mod's surroundings. Otherwise, unrestricted access is available before and after the run day. Hardhats should always be worn when working near the reactor.
11. Use dwscope as before to review any desired plasma diagnostics after the run day has concluded.
 1. Note that data can also be programmatically accessed through various MDSplus APIs for different languages.

5. Calibration of HIREXSR Locked Mode Data Using THACO

1. Use The HIREXSR Analysis Code (THACO) to invert HIREXSR data, which is line-integrated¹². Reference and detailed breakdown for all of these steps can be found online in the unpublished THACO Manual on the MIT Plasma Science and Fusion Center (PSFC) online library. This section covers first-time setup and launching of THACO, followed by the calibration process.
2. Follow the instructions on the Alcator C-Mod wiki page for THACO to set up THACO for first-time use on a machine connected to the PSFC network. You may also need to request write access to the SPECTROSCOPY tree from the network administrator.
3. Enter 'idl' into a command line from to launch the IDL command line interface.
4. From IDL, enter '@thaco.bat' to launch THACO.
5. Identify a locked mode to be used for calibration of the data.
 1. Open a web browser and navigate to the PSFC logbook.
 2. Click the "custom query" button to bring up a search page.
 3. In the custom query textbox, enter "SHOT LIKE '1yymmdd%%%' and TEXT LIKE '%locked mode%'", where yymmdd is the year/month/day of the run day, to bring up log entries containing the text locked mode.
 4. Determine the shot number of the locked mode from the log entries, and take note of the locked mode start/end times.
 5. Note that having a locked mode baseline is not strictly necessary for all diagnostics, like those involving line ratios like determining the electron temperature¹³, but is highly recommended since the Bragg angle may shift from day to day due to the crystal lattice expanding/contracting¹⁴.
6. In the THACO GUI, enter the locked mode shot number to the text field "(ACTIVE) SHOT", and press enter.
7. Press the button "LAUNCH W_HIREXSR_CALIB" and launch the calibration widget.
 1. In the window that pops up, make sure that the field labeled "SHOT" contains the locked mode shot number, and take note of the number in "MODULE". Press enter after any changes are made to any field.
 2. Click the "LOAD" button in the top third of the window and wait for data to be loaded.
 3. Click "LOAD" in the middle third of the window and wait for more data to be loaded.
 4. If data is successfully loaded and the fit ellipses look good, repeat the calibration step with a different number in the "MODULE" field (1-4), as the locked mode shot has already been calibrated.
 5. If all modules (1-4) have already been calibrated, skip the rest of the calibration and detector alignment steps since the shot has already been calibrated, and proceed directly to Section 6.
8. Begin spectral fitting by selecting the appropriate option in the upper-right hand corner of the window. Only H-like and He-like Ar and Ca spectra are supported out of the box currently.
 1. Set the "t1 =" and "t2 =" fields to the locked mode start/end times respectively that are mentioned in the logbook.
 2. Move the "FIT LOW" and "FIT HIGH" sliders until the region of fit, denoted by dashed white lines superimposed on the spectrum in the upper-left, contains only the region where the spectral lines of interest are visibly resolved.
 3. Click the "FIT/SAVE SPECTRA" button and wait for the fitting process to finish.
 4. Once the fitting process is finished, used the "SPEC" slider or the left/right arrows next to it in the middle third of the GUI to visually inspect all of the spectral fits.
 5. Remove any bad or outlier fits by checking the "BAD" checkbox next to the "SPEC" slider. Reference the works found in Step 1.3 for comparison against known spectra. For example, He-like Ca spectra will resemble **Figure 10**.
9. Begin ellipse fitting by selecting the desired line (w, x, y, z) from the bottom third of the GUI.
 1. Click the "FIT ELLIPSES" button and wait for ellipses to be fit to the spectral fits.
 2. Move the "LOW", "HIGH", and "OUTL" sliders until the ellipse fit visually matches the spectra. The ellipses are fit with a non-linear least squares method MPFIT¹⁵, which can be finicky.
 3. Click the "SAVE ELLIPSES" button when done, and repeat the process with the next desired line.
 4. When all lines have been fit, change the "MODULE" to a different module (1-4) that has not been calibrated yet and press enter, and proceed again from step 5.7.1.
 5. When all modules have been calibrated, click the "QUIT" button (not the 'x') to close the widget.
10. Press the button "LAUNCH W_HIREXSR_DET_ALIGN" to launch the detector alignment widget.
 1. In the "SHOT" field, enter the shot number of a recent known locked mode which has already been calibrated and press enter. Take note of the "MODULE" field.
 2. Click the "LOAD" button and wait for the data to load.
 3. In the lower-left corner, write down all the slider values in the "DETECTOR POSITION" panel.
 4. In the "SHOT" field, enter the shot number of the locked mode being calibrated and press enter.
 5. Click the "LOAD" button and wait for the data to load.
 6. Enter the values written down earlier into the "DETECTOR POSITION" panel, pressing enter after each change.
 7. Change the values in the "DETECTOR POSITION" panel, either through the sliders or by manually changing values in the textboxes, until all or most of the circular residuals lie within the green bar.
 8. Change the "MODULE" field to a module (1-4) that has not been aligned yet and press enter. Then proceed from step 5.10.1.
 9. When all modules have been aligned, click the "QUIT" button (not the 'x') to close the widget.

10. Calibration is now done; proceed to Section 6 with the locked mode shot.

6. Advanced Analysis of HIREXSR Data Using THACO

1. Use The HIREXSR Analysis Code (THACO) to invert HIREXSR data, which is line-integrated¹¹. Reference and detailed breakdown for all of these steps can be found online in the unpublished THACO Manual on the MIT Plasma Science and Fusion Center (PSFC) online library. This section covers the actual inversion process to view profile data.
2. Determine the shot number for the shot of interest.
3. From the THACO GUI, set the field "(ACTIVE) SHOT" to the shot number, and press enter. The GUI should acknowledge the change in the log on the bottom.
4. Choose the spectral line of interest, set the field "LINE" to the line number of interest. For argon, this will usually be 2 for the He-like z line, and 3 for the H-like Iya1 line.
 1. Click "LIST THACO LINE NUMBERS" to list all of the line numbers available.
5. Click on the "BINNING" tab in the top part of the GUI.
 1. Click "CHECK THT AVAILABILITY" to check the THACO Tree (THT) availability. The bottom part of the GUI should log all available THACO trees.
 2. Set the field "new THACO tree (THT) number" to the first number not listed in the availability.
 3. Click the "CREATE" button to create a new THT so previous analysis is not overwritten.
 4. Click "CHECK THT AVAILABILITY" again to refresh the list of available THTs.
 5. Change the "THT" field next to the "(ACTIVE) SHOT" field to the newly created THT number, and press enter. The GUI log should acknowledge this action.
6. If the current shot is not a locked mode, click the "CALIB" tab in the top part of the GUI.
 1. Change the "Calibration Data From Shot" to the locked mode to be used to calibrate the data.
 2. Press the "COPY" button to copy over the calibration.
7. Click the "BINNING" tab again.
 1. Consult the THACO manual for instructions on making custom binnings.
 2. To copy binning from a previous analysis, enter the shot/THT into their respective fields (pressing enter after each change) in the panel with the "COPY" button.
 3. Copy over the binning: Select "BRANCH A" and click "COPY", then select "BRANCH B" and click "COPY" again.
8. Click the "PROFILES" tab in the top part of the GUI.
 1. Consult the THACO manual for instructions on how to use the advanced features present in this section.
 2. Otherwise, enter the shot/THT from a previous analysis into their respective fields (pressing enter after each change) in the top panel.
 3. Click the "LOAD RHO" button, followed by the "LOAD GOOD" button.
9. Click the "RUN THACO" button, and THACO will begin the inversion process. This may take a couple minutes.
10. Note that THACO is actually going through a series of independent steps during this process: running a multi-Gaussian fit on the spectra to calculate moments of various lines, using those moments to calculate line-integrated profile data, then inverting the line-integrated data through a least-squares method. Intermediate outputs from these steps, useful for troubleshooting, can be found in the moments and profiles widgets. Interested users are encouraged to look through the THACO manual for more information about these steps and how to use these widgets for finer-grained control over the inversion process.
11. Once the inversion process finishes, from the "PROFILES" tab click "LAUNCH_W_HIREXSR_PROFILES" to visually inspect the profiles.
 1. Press the "LOAD" button in the "Tree I/O" panel at the bottom and wait for the data to load.
 2. If the automated process fails, find "DO INVERSIONS FOR" and click "ALL" to quickly redo all the inversions.
 3. Manually inspect the inverted profiles on the right by using the "TIME" slider at the bottom to change frames.
 4. If there are any inverted profiles that appear to be wrong (e.g., negative temperatures, unphysical gradients towards the edge, etc.), use the +/- buttons next to "CH#" to select outlier channels on the left, and uncheck the "GOOD" option to remove them from the inversion step.
 1. Note that emissions tend to be weaker towards the edge so uncertainty is higher; however, the inverted temperature should still go to a small (not necessarily) zero value at the edge.
 5. Find "DO INVERSIONS FOR" and click "CURRENT" to invert the profile for the current frame. Repeat removing outliers until the inverted profile seems correct.
 6. Press "SAVE" after the data seems satisfactory.
 7. Use the profiles widget to inspect the data.
12. If desired, click "LAUNCH_W_HIREXSR_COMPARE" in the "COMPARE" tab to compare profiles constructed from different spectral lines. A common scenario where this is useful is when the plasma core temperature becomes hot enough for argon H-like emission to overtake the He-like emission.
13. Note that data can also be programmatically accessed through various MDSplus APIs for different languages. Refer to the THACO manual for the relevant paths.

Representative Results

A representative data sample from the pixel detector for one time bin for the He-like argon spectrum is shown in **Figure 17**. The spectral lines, bent into an elliptical shape by the spherical crystal, are clearly visible. The top detector has a broken detector panel, and there are some

dead pixels scattered across all of the detectors. Data from the broken detector panel should be ignored. Slices from the detector showing the measured spectra and results of the spectral fitting done by THACO over a single chord are shown in **Figure 18** and **Figure 19**. The resulting line-integrated profile data is shown in **Figure 20**.

An example of an inverted plasma temperature and toroidal velocity profile created by THACO from the He-like argon lines can be seen in **Figure 21**. The measured ion temperatures from HIREXSR agree with independent diagnostics in other measurement channels¹. Using argon, a recycling impurity, allows the ion profiles to be measured over the entire evolution of the plasma. This is critical for transport studies such as in Rice *et al.* 2013¹¹, which study plasma evolution over time scales longer than the impurity confinement time. If the detectors were instead positioned to measure a transient impurity, such as calcium, HIREXSR would provide transient profile data. See Howard *et al.* 2011¹⁰ for such a study.

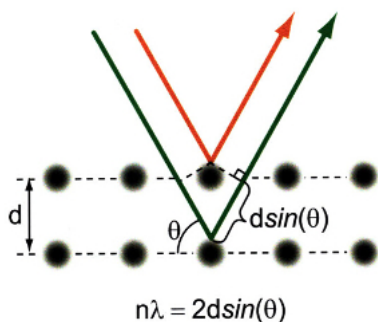


Figure 1. Illustration of Bragg Reflection. Incoming rays will reflect and constructively interfere based on their angle of incidence and wavelength. [Please click here to view a larger version of this figure.](#)

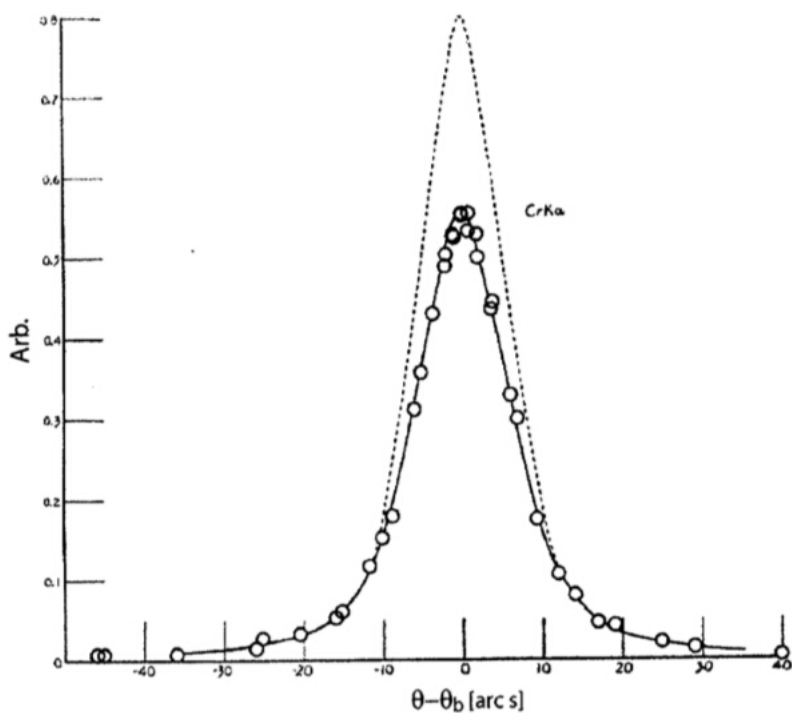


Figure 2. A Rocking Curve for a Calcite Crystal. The black curve is the best fit to the observed data, while the dotted line is the idealized case where there is no absorption.

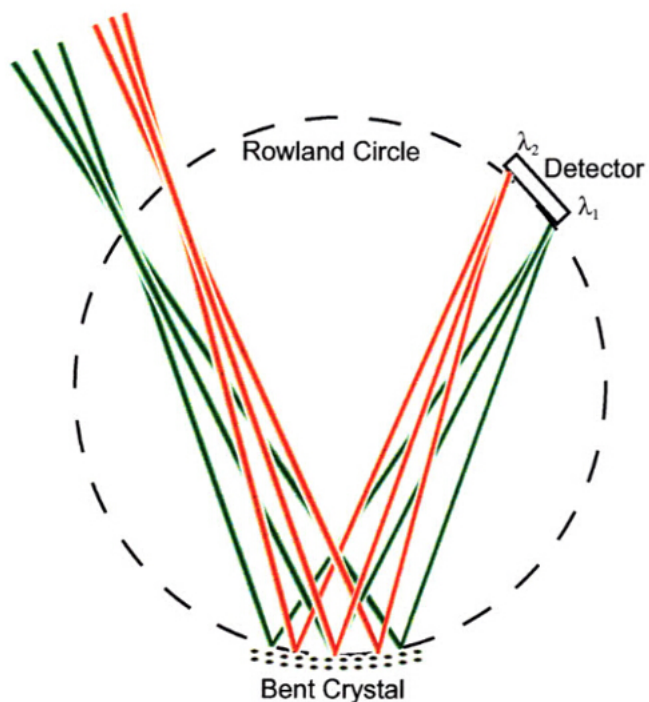


Figure 3. A Johann Spectrometer with a Bent Crystal. Incoming rays incident on the same location on the circumference of the circle have the same angle of incidence on the crystal and end up on the same location on the detector. [Please click here to view a larger version of this figure.](#)

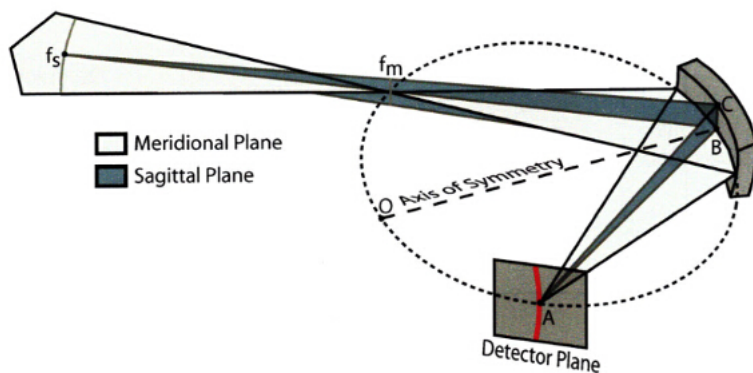


Figure 4. A Johann Spectrometer with a Spherically Bent Crystal. The spherical bending of the crystal allows for spatial resolution along the meridional plane, so spectra are captured along multiple line-averaged chords through the plasma. [Please click here to view a larger version of this figure.](#)

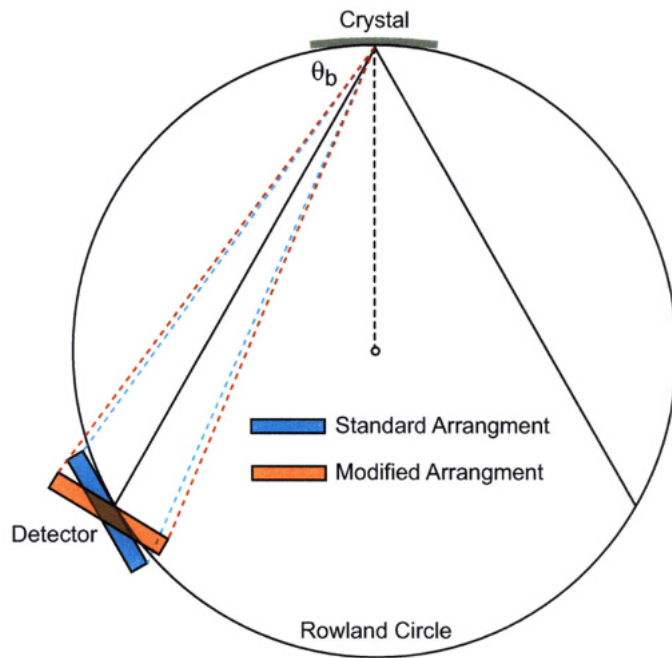


Figure 5. The detector-crystal alignment used in HIREXSR. In HIREXSR, the detector is angled slightly from the standard arrangement to allow for a larger range of wavelengths to be measured. [Please click here to view a larger version of this figure.](#)

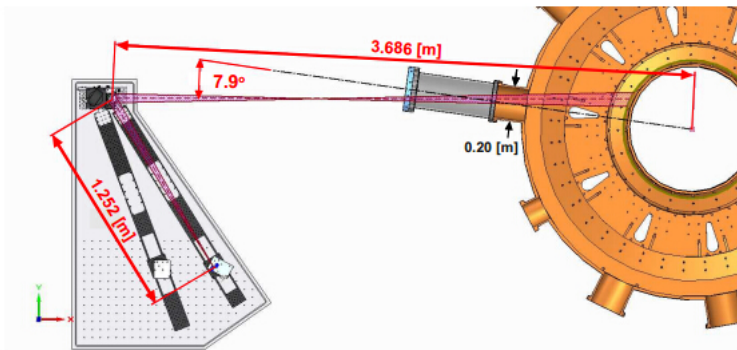
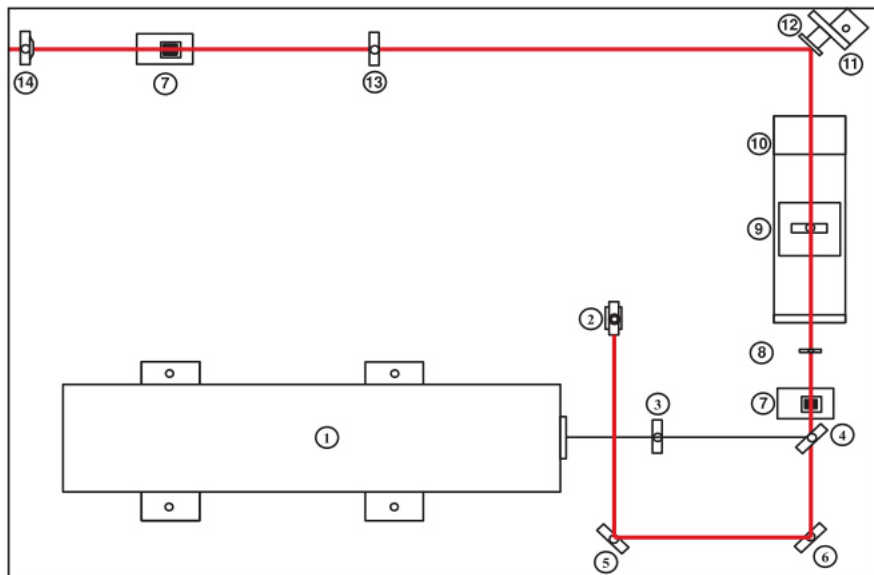


Figure 6. Top-down CAD View of HIREXSR. This CAD drawing shows the relative positions of the two detector arrays and the spectrometer crystal to the tokamak vacuum vessel, which contains the plasma. The sightline of the spectrometer is angled slightly off-axis to allow toroidal rotation to be measured through the Doppler shift.



- | | |
|--|--|
| 1. Nd:YAG laser (10 Hz rep rate, 1064 nm, 680 mJ/pulse) | 8. Mechanical Iris (1 inch max aperture) |
| 2. Diode Alignment Laser (633 nm) | 9. Plano-Convex Converging Lens (f = 1146 mm, Fused Silica) |
| 3. Plano-Concave Diverging Lens (f = -500 mm, BK7 Glass) | 10. Linear Translation Stage (200 mm travel) |
| 4. Mirror (BK7 Glass, R~99% @ 1064 nm, T~80% @ 633 nm) | 11. Motorized Mirror Mount (+/- 97 mrad) |
| 5. Silvered Glass Mirror | 12. Piezo Electric Mirror Mount (Tip/Tilt 4 mrad) |
| 6. Silvered Glass Mirror | 13. Plano-Convex Converging Lens (f = 1146 mm, Fused Silica) |
| 7. Photodiode Housing/Photodiode | 14. Wedge Prism (10 degrees @ 1064 nm) |

Figure 7. Layout of Optical System. This figure shows the layout of the optical system for the laser blow-off system from Howard *et al.*¹⁰

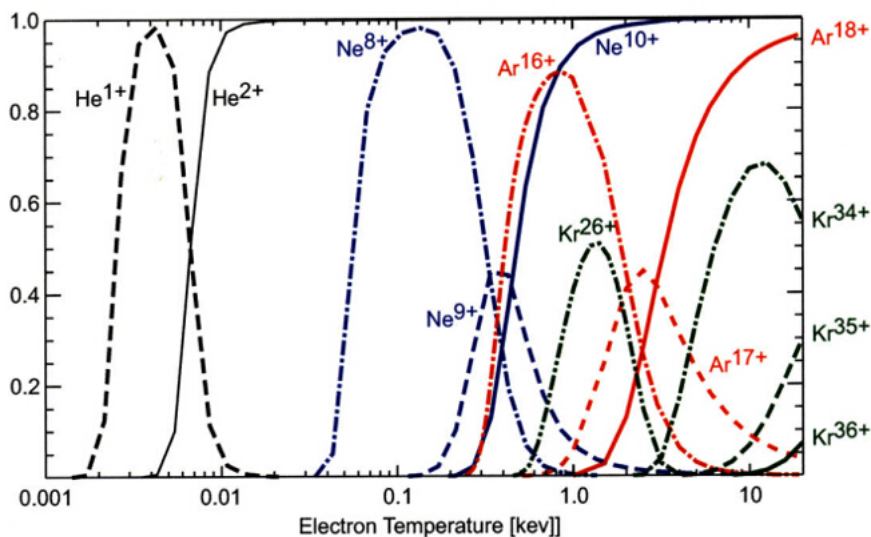


Figure 8. Fractional Charge State Abundance for Various Noble Gases. This plot shows the fractional charge state abundances for various noble gases in coronal equilibrium. Fully stripped states are in shown with solid lines, H-like with dashed, He-like with dash-dot and Ne-like with dash-dot-dot. [Please click here to view a larger version of this figure.](#)

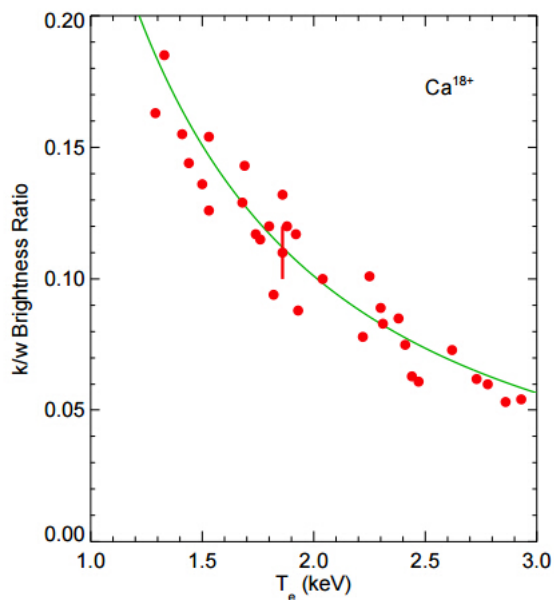


Figure 9. Ca^{18+} k/w Brightness Ratios. The measured chord-averaged brightness ratio of the dielectronic satellite k to the resonance line w in He-like Ca^{18+} (red dots) compared to the theoretical curve (green line).

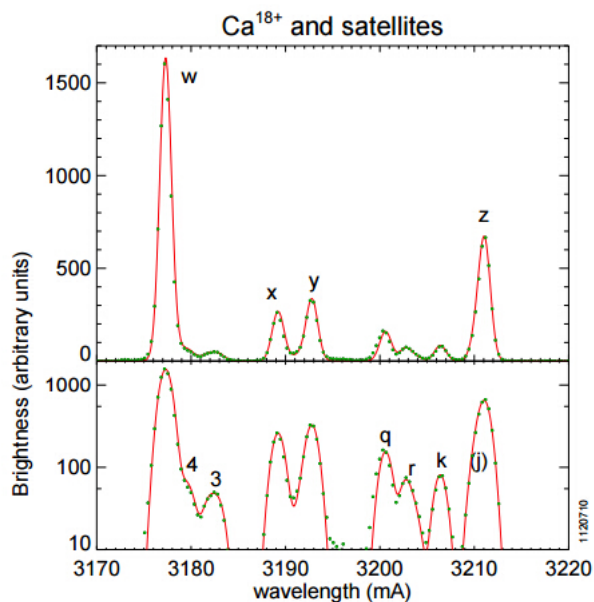


Figure 10. Measured He-like Ca^{18+} Spectrum. The measured He-like Ca^{18+} (w, x, y, and z) spectrum with satellites (most prominent '4', '3', q, r and k) is shown by the dots. A synthetic spectrum calculated with collisional-radiative modeling indicated by the solid line.

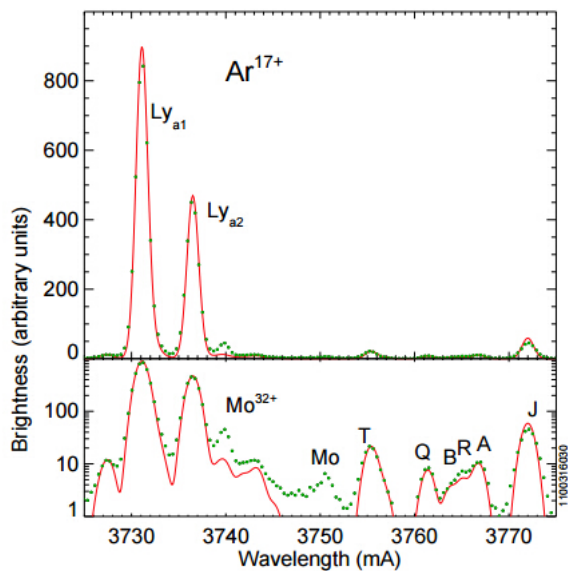


Figure 11. Measured H-like Ar^{17+} Spectrum. The measured spectrum of the Ar^{17+} Ly_{α} doublet and nearby satellites (green dots), with synthetic spectrum (red line). Note the overlap between the Mo^{32+} line and the $Ly_{\alpha 2}$ line.

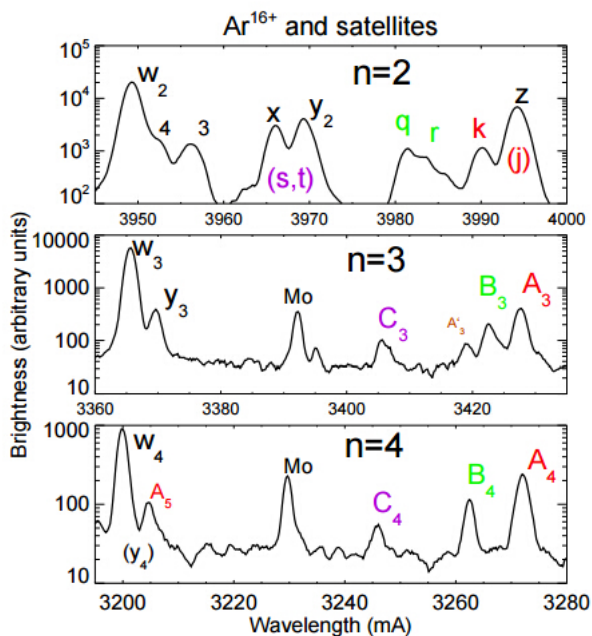


Figure 12. Measured He-like Ar^{16+} Spectrum. Measured X-ray spectra in the vicinity of the Ar^{16+} w resonance lines. Note the log scale.

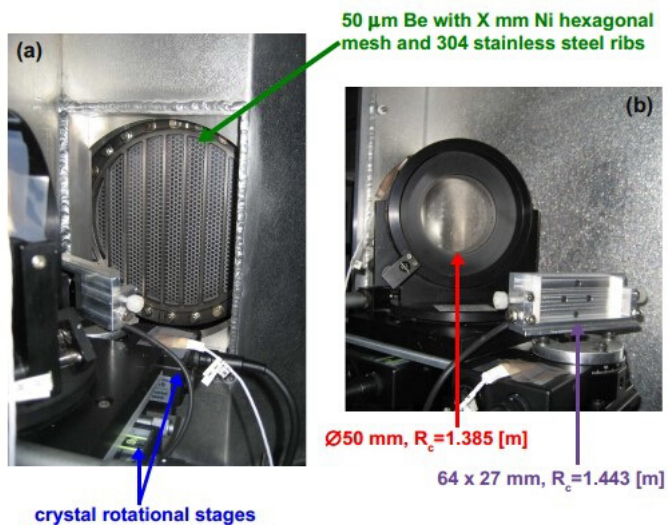


Figure 13. Internal View showing Crystals and Be Window. The beryllium window (a) and crystals (b) are displayed as viewed from within the housing. The Be window is labeled with green, the spherical crystal with red, and the rectangular crystal with purple.

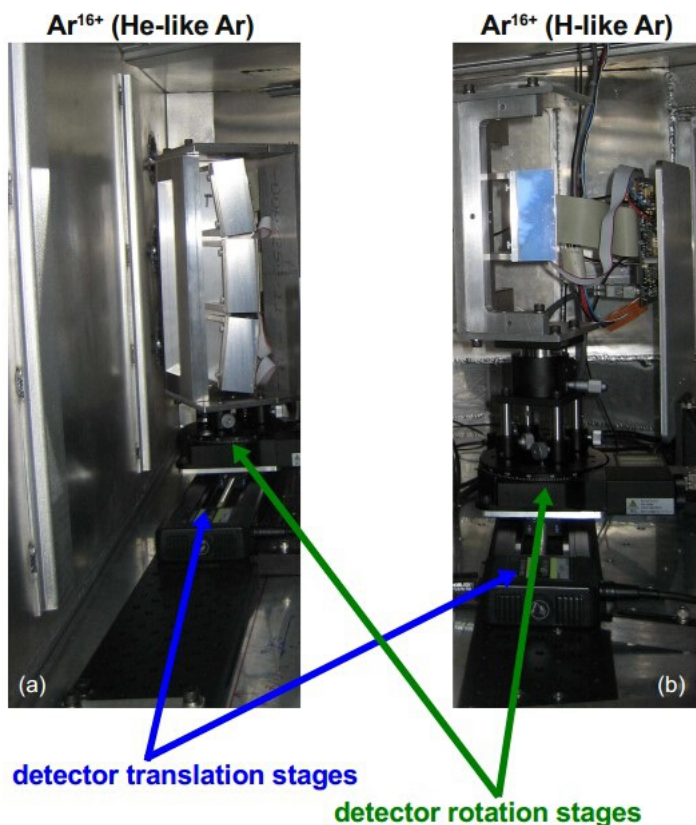


Figure 14. Internal View Showing Detectors. The three detector array for He-like spectra is shown on the left in (a), and for H-like spectra is shown on the right in (b). The three detectors used for He-like spectra allow for the capture of spectra from the core and edge of the plasma simultaneously.

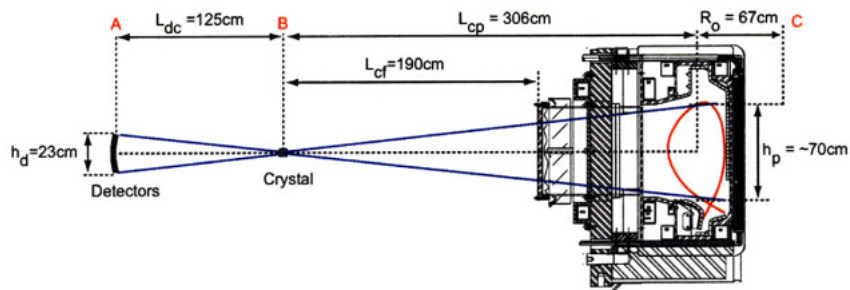


Figure 15. Side View of HIREXSR. This diagram illustrates the relative distances of the detectors, crystals, and the tokamak. [Please click here to view a larger version of this figure.](#)

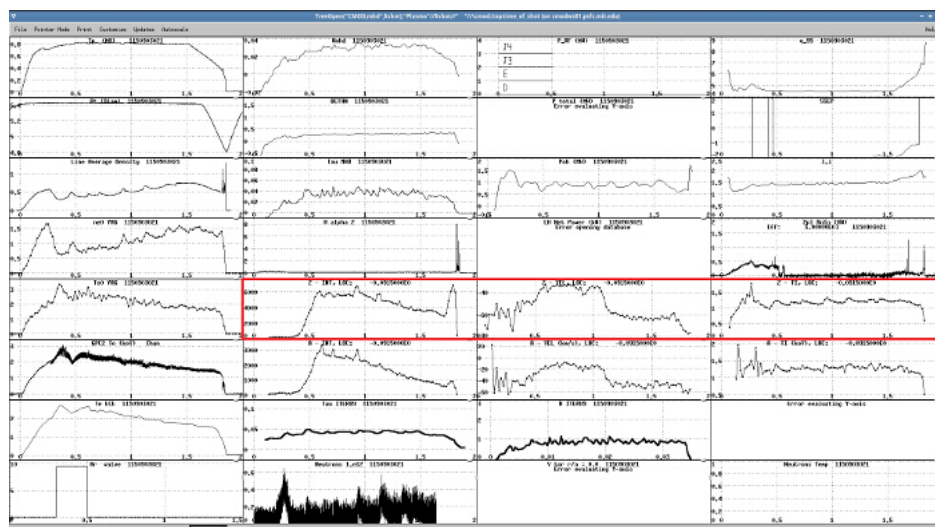


Figure 16. Example View of dwscope. This figure shows a screenshot of an instance of dwscope. Line-integrated data from HIREXSR is highlighted by the red box. [Please click here to view a larger version of this figure.](#)

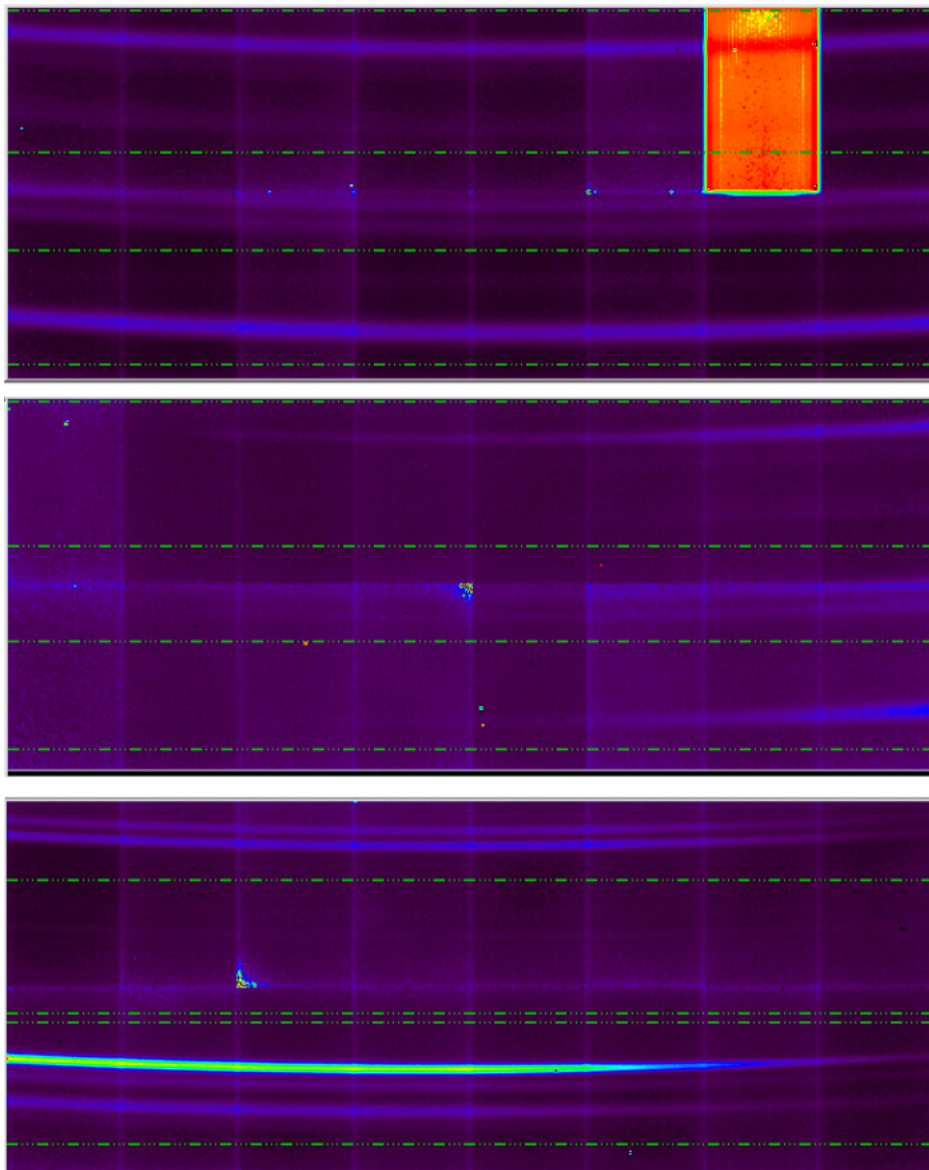


Figure 17. Example Detector Output. This figure shows example raw data collected by the detectors over a single time bin for He-like (top, middle) and H-like (bottom) argon spectra. The y-axis corresponds to wavelength, and the x-axis to meridional angle. The spectral lines, bent into an elliptical shape by the spherical crystal, are clearly visible. The top (1x gain) and bottom (2x gain) spectra are from the core, and the middle spectrum (8x gain) is from the edge. The dotted green lines separate different regions for the spectral fitting code. The top detector has a broken detector panel, and there are some dead pixels scattered across all of the detectors. [Please click here to view a larger version of this figure.](#)

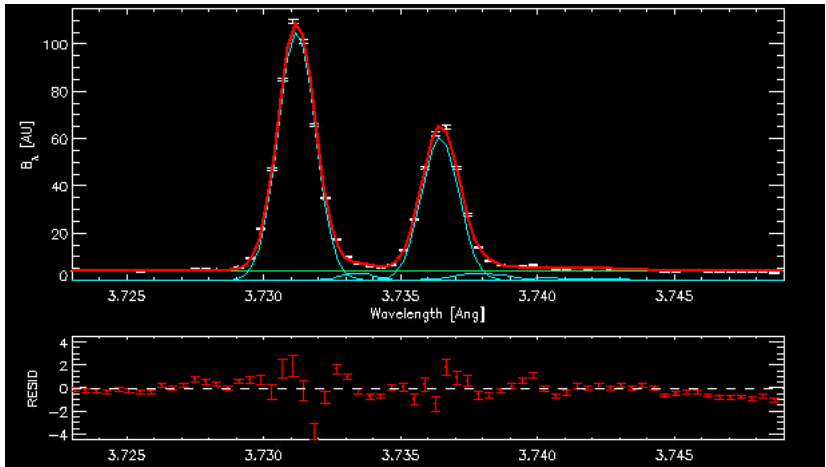


Figure 18. Example Collected H-like Spectra. Measured line-averaged brightness over the argon H-like spectrum for a single chord and time bin (top, white), corresponding to a single column of pixels in the bottom detector in **Figure 17**. The removed background is shown in green, and a multi-Gaussian fit is shown in cyan. The total fit composite spectrum is shown by the red line, and the residuals are in the bottom figure. Note the agreement with **Figure 11**.

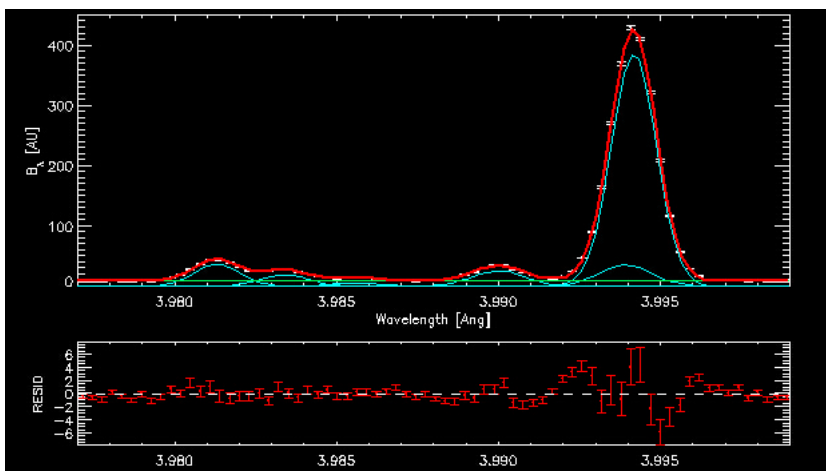


Figure 19. Example Collected He-like Spectra. Measured line-averaged brightness over the argon He-like spectrum for a single chord and time bin (top, white), corresponding to a single column of pixels in the top detector in **Figure 17**. The removed background is shown in green, and a multi-Gaussian fit is shown in cyan. The total fit composite spectrum is shown by the red line, and the residuals are in the bottom figure.

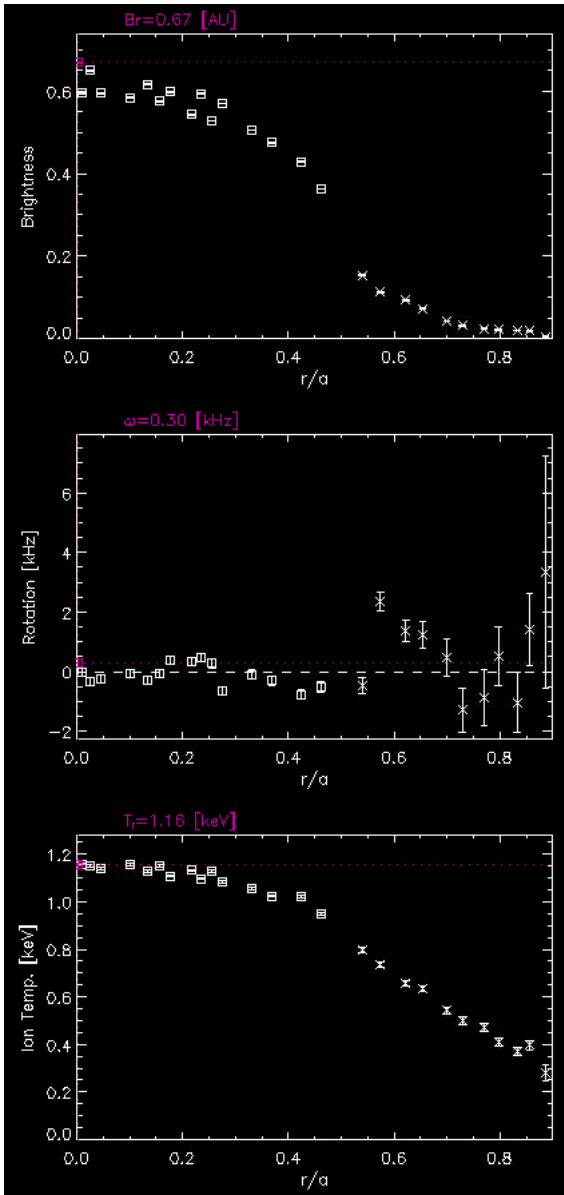


Figure 20. Example Line-Integrated Profile. This figure shows an example of the line-integrated data generated by THACO from the results of the line fitting. It needs to be tomographically inverted to return the full profile.

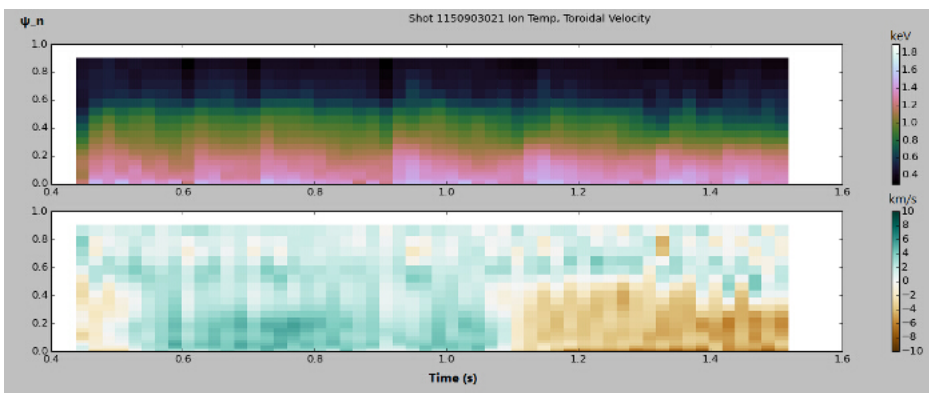


Figure 21. Example Inverted Plasma Profiles. This figure shows example data that has been inverted by THACO to produce temperature and toroidal rotation profiles. HIREXSR allows for both spatial resolution (along the y-axis) and time resolution (along the x-axis). [Please click here to view a larger version of this figure.](#)

Sensor Type	Reverse biased silicon diode array
Sensor Thickness	320 μm
Pixel Size	172 μm \times 172 μm
Format	487 \times 195 = 94,965 pixels
Area	83.8 mm \times 33.5 mm
Dynamic Range	20 bits (1:1,048,576)
Count Rate Per Pixel	$> 2 \times 10^6$ X-rays/sec
Energy Range	3-30 keV
Energy Resolution	\sim 500 keV
Adjustable Threshold Range	2-20 keV
Readout Time	2.7 msec
Maximum Frame Rate	300 Hz
Point Spread Function	1 pixel
External Trigger/gate	5 V TTL
Power Consumption	15 W
Dimensions	275 \times 146 \times 85 mm
Weight	1 kg

Table 1. Detector Specifications. This table lists detector specifications relevant to the design of HIREXSR.

Discussion

The data generated by this technique can be used in a wide variety of experimental studies. Ion temperature and toroidal velocity profiles can be used in a wide range of transport studies, including intrinsic self-generated plasma rotation and non-local perturbative effects. Measuring spectra of injected impurities through laser blow-off can also provide important information about the transport of impurities in the plasma, as was done in Howard *et al.* 2011¹⁰. At this time, no other plasma diagnostic can provide time and spatially resolved ion profile data from the plasma core¹, making X-ray imaging spectroscopy a novel method for probing plasma behavior.

The most critical step in the protocol is the identification of spectral lines in the wavelength region of interest. It is important that the lines being observed are strong to provide good counting statistics, and resolved from both each other and other satellite lines. The relative strength of these lines may change dramatically with different temperatures, and quantum processes like dielectric recombination can have measurable effects.

If the spectral lines are weak, it may be possible to improve their strength by introducing more of the measured impurity. If a different range of wavelengths is of interest, the detectors simply need to be moved along the Rowland circle, as long as the Bragg angle is still between greater than 45° to avoid diverging rays and less than 80° to prevent interference between incoming and reflected photons. The frame rate of the detectors can also be changed to be faster or slower. The detector does not count photons during the readout time, so the fraction of captured photons increases with longer frames, allowing for better statistics in the obtained data.

The spectrometer-reactor interface should be leak tight to 10⁻⁹ std cc/sec and capable of sustaining a differential pressure of 1 atm to either side. The beryllium window is the ideal choice for this interface due to its high strength and good X-ray transmission coefficient, which is around 40% for 3.1 keV X-rays. The helium atmosphere maintained within the housing of HIREXSR to reduce X-ray attenuation to around \sim 1% of incoming rays. The constant pumping ensures that no air is leaking into the housing and contaminating the local atmosphere. These systems should be double-checked for leaks to ensure X-rays make it to the detectors.

A vacuum chamber would be the ideal housing for the spectrometer. However, such a chamber is very expensive and impractical to maintain for such a large spectrometer. Future improvements could focus on using new techniques or recent innovations to create a spectrometer-reactor interface and local atmosphere that minimizes X-ray absorption, or attempt to make current or similar designs cheaper and more viable.

The technique is limited by its temperature requirements, as the plasma needs to be hot enough to ionize the impurity of interest, but cool enough to allow for recombination. In addition, H-like and He-like ionization states are preferred since their spectra are much simpler and easier to characterize. This means it is difficult to get data from the cooler edge of the plasma, and it may require physical reconfiguration of the machine to get useful data from plasmas across the temperature range of the tokamak. Additionally, the technique is somewhat limited by the necessity of running calibration shots due to the thermal expansion of the spectrometer crystal. This could be improved in the future with better temperature controls on the crystal, or other novel calibration techniques.

Disclosures

The authors have nothing to disclose.

Acknowledgements

The authors would like to thank Matt Reinke and the Alcator C-Mod team for designing, building, and testing HIREXSR. This work was supported by DOE Contract Nos. DE-FC02-99ER54512 and DE-AC02-76CH03073.

References

1. Reinke, M. L., *et al.* X-ray imaging crystal spectroscopy for use in plasma transport research. *Rev. Sci. Instrum.* **83** (11), 113504 (2012).
2. Hill, K. W., *et al.* Development of a High Resolution X-Ray Imaging Crystal Spectrometer for Measurement of Ion-Temperature and Rotation-Velocity Profiles in Fusion Energy Research Plasmas. *Plasma Fusion Res.* **2** S1067-S1067 (2007).
3. Greenwald, M., *et al.* 20 years of research on the Alcator C-Mod tokamak. *Phys. Plasmas.* **21** (11), 110501 (2014).
4. Rice, J. E., *et al.* X-ray observations of medium Z H- and He-like ions with satellites from C-Mod tokamak plasmas. *J. Phys. B.* **48** (14), 144013 (2015).
5. Ince-Cushman, A. Rotation studies in fusion plasmas via imaging X-ray crystal spectroscopy *Rev. Sci. Instrum.* **79**, 10E302 (2008).
6. Zachariasen, W. H. *Theory of X-Ray Diffraction in Crystals.* Courier Corporation (2004).
7. Johann, H. H. Die Erzeugung lichtstarker Röntgenspektren mit Hilfe von Konkavkristallen. *Zeitschrift für Physik.* **69** (3-4), 185-206 (1931).
8. Wang, E., *et al.* Calculation of the Johann error for spherically bent x-ray imaging crystal spectrometers. *Rev. Sci. Instrum.* **81** (10), 10E329 (2010).
9. Eikenberry, E., *et al.* PILATUS: a two-dimensional X-ray detector for macromolecular crystallography. *Nucl. Instr. Meth. Phys. Res. A.* **501** (1), 260-266 (2003).
10. Howard, N. T., Greenwald, M., & Rice, J. E. Characterization of impurity confinement on Alcator C-Mod using a multi-pulse laser blow-off system. *Rev. Sci. Instrum.* **82** (3), 1-6 (2011).
11. Rice, J. E. *et al.* Non-local heat transport, rotation reversals and up/down impurity density asymmetries in Alcator C-Mod ohmic L-mode plasmas. *Nucl. Fusion* **53**, 033004 (2013).
12. Reinke, M. L., Podpaly, Y., Gao, C., & Science, P. *Operation and Validation of The HIREXSR Analysis COde MIT-Plasma Science and Fusion Center Alcator C-Mod.* at <http://library.psfc.mit.edu/catalog/reports/2010/11rr/11rr009/11rr009_full.pdf> (2013).
13. Rosen, A. S., Reinke, M. L., Rice, J. E., Hubbard, A. E., & Hughes, J. W. Validation of x-ray line ratios for electron temperature determination in tokamak plasmas. *J. Phys. B.* **47** (10), 105701 (2014).
14. Delgado-Aparicio, L. F., *et al.* In-situ wavelength calibration and temperature control for the C-Mod high-resolution X-ray crystal imaging spectrometer. *Bull. Am. Phys. Soc.* **55** (2010).
15. Markwardt, C. B. *Non-linear Least Squares Fitting in IDL with MPFIT.* at <<http://arxiv.org/abs/0902.2850>> (2009).